Study of the low-lying negative-parity states in ^{11}Be using the ^{12}B$(d,^3$He$)^{11}$Be reaction

J. Chen,[1, *] K. Auranen,[1] M. L. Avila,[1] B. B. Back,[1] C. R. Hoffman,[1] D. Gorelov,[2, 1]

B. P. Kay,[1] S. A. Kuvin,[3, 1] Q. Liu,[4] D. G. McNeel,[3, 1] T. L. Tang,[1] D. Santiago-Gonzalez,[1]

J. P. Schiffer,[1] R. Talwar,[1] J. Wu,[1] G. Wilson,[5, 1] C. X. Yuan,[6] and H. L. Zang[4]

[1]*Physics Division, Argonne National Laboratory, Argonne, Illinois 60439, USA*
[2]*University of Manitoba, Department of Physics and Astronomy,*
Allen Building, Winnipeg, MB R3T 2N2, Canada
[3]*Department of Physics, University of Connecticut, Storrs, Connecticut 06269, USA*
[4]*School of Physics and State Key Laboratory of Nuclear Physics and Technology, Peking University, Beijing 100871, China*
[5]*Department of Physics and Astronomy, Louisiana State University, Baton Rouge, Louisiana 70803, USA*
[6]*Sino-French Institute of Nuclear Engineering and Technology, Sun Yat-Sen University, Zhuhai 519082, China*
(Dated: May 16, 2019)

The p-wave neutron configuration of the low-lying negative-parity states in ^{11}Be were studied using the ^{12}B$(d,^3$He$)^{11}$Be reaction in inverse kinematics. The $1/2_1^-$ state at 0.32 MeV, the $3/2_1^-$ state at 2.56 MeV and one or both of the doublets including the $5/2_1^-$ state at 3.899 MeV and the $3/2_2^-$ state at 3.955 MeV were populated in the present reaction. Spectroscopic factors were determined from the cross sections using a distorted wave Born approximation method. The $0p_{3/2}$ proton removal strengths were well described by the shell model calculations using the YSOX interaction.

I. INTRODUCTION

In the light nuclei, the structure of the Be isotopes provides a great testing ground in some of the simplest nuclei for the approximations made in the shell-model, the cluster model and the Nilsson model (where "deformation" must arise from only the very few p-shell nucleons), as well as the less model-dependent *ab-initio* calculations. The strong clustering in ^{8}Be was evidenced by the ground state rotational band and the enhanced E2 transition. This naturally suggests that deformation degree of freedom will play an important role in the structure of the Be isotopes. In ^{11}Be, this was confirmed by some indications for the rotational bands with $K^\pi = 1/2^+, 1/2^-$ and $3/2^-$ [1, 2]. In a recent work by Macchiavelli *et al.* [3], they interpreted the structure of Be isotopes within the Nilsson strong coupling limit and obtained good agreement with most available structure and reaction data. To fully complete the picture of Be isotopes, we study the proton spectroscopic factors of the ^{12}B$(d,^3$He$)^{11}$Be reaction. The ground state of ^{11}Be is usually interpreted as a halo state, with the ^{10}Be core inside a cloud of a loosely bound valence neutron. Based on this picture, ^{11}Be low-lying states were also understood in the shell-model single-particle framework. The famous orbital inversion of $0p_{1/2}$ and $1s_{1/2}$ single-particle orbital was observed in ^{11}Be compared to $N = 7$ isotone ^{12}B. Via proton removal from ^{12}B, the evolution of the low-lying states from ^{12}B to ^{11}Be will be studied.

The duality of the collective and single-particle descriptions of the atomic nucleus structure has been confirmed by recent experimental work [4], and the present system provides a unique testing ground for it. Further, the less model-dependent *ab-intio* calculations,

which aspire to be able to predict rotational band structure in light nuclei, could be tested with descriptions of ^{11}Be.

The low-lying negative-parity states have been studied using the ^{9}Be$(t,p)^{11}$Be reaction [5] and β-decay of ^{11}Li [6–8]. These works understood structure of the low-lying negative-parity states in the shell-model framework. From the viewpoint of molecular structure, the negative-parity states with $\nu(2p-2h)$ configuration were understood to be the members of the molecular band with two alpha center [1]. The ^{9}Be$(^{13}$C,^{11}C$)^{11}$Be transfer reaction on the well-developed $\alpha : n : \alpha$ structure of ^{9}Be(g.s.) populated the molecular structure of ^{11}Be and suggested a long rotational band $K^\pi = 3/2^-$ built on the 3.96-MeV $3/2^-$ state, which extends to $13/2^-$ state [2]. Another band is believed to be headed with the relatively bound $1/2_1^-$ states and terminated by the $7/2^-$ state, which is currently not well studied.

In the present work, we test various descriptions of ^{11}Be using the ^{12}B$(d,^3$He$)^{11}$Be reaction, including effective-interaction shell-model, Nilsson-model, VMC calculations and No-core shell-model calculations. Studies on ^{12}B indicates the dominance of p-orbital neutron configuration [9–11]. With removal of one $0p_{3/2}$ orbital proton, the negative parity state in ^{11}Be are possibly populated. The ^{12}B$(d,^3$He$)^{11}$Be reaction is a probe of the neutron p-wave strength in ^{11}Be. The present ^{12}B$(d,^3$He$)^{11}$Be reaction solidifies the low-lying negative-parity states and determines if there are any strengths within p-shell orbitals. Negative-parity states with large $\nu(2p-2h)$ configuration will not be strongly populated in this reaction, although allowed by the transferred angular momentum. An overall interpretation of the low-lying negative-parity states will be presented, which shed light on the mixing between sd- and p-shell as well as the structures of the p-shell states in ^{11}Be.

---

* jie.chen@anl.gov

II. EXPERIMENT

The ^{12}B(d,^{3}He)^{11}Be reaction was carried out in inverse kinematics, at the Argonne National Laboratory ATLAS In-Flight Facility. The 12 MeV/u ^{12}B secondary beam was produced using the neutron adding reaction on a ^{11}B primary beam at 13.5 MeV/u. This beam with an intensity of 200 pnA bombarded a 3.7-cm long D_2 gas cell at a pressure of 1400 mbar and temperature of 90 K. The resulting ^{12}B was approximately 2×10^5 particle per second and had very little contamination (less than 5%). Data from ^{11}B(d,^{3}He) at 13.5 MeV/u was also collected at the beginning of the experiment to serve as an energy calibration and provided check of the analysis procedure.

The outgoing charge particles were analyzed by the HELical Orbit Spectrometer (HELIOS) [12, 13] with a magnetic field strength of 2.3 T and the experimental setup resembled that shown in Fig. 2 of Ref. [14]. The ^{12}B ions bombarded a Deuterated polyethylene $(CD_2)_n$ target of thickness 400 μg/cm^2 placed within the uniform magnetic field, and its position was defined as $Z = 0$ cm. The ^{3}He particles from the reaction were transported to an array of 24 position-sensitive silicon detector (PSDs) that was positioned downstream of the target covering a range of 72 cm$< Z <$107 cm. A silicon $\Delta E - E$ telescopes was placed at $Z = 42$ cm to identify the ^{9}Be, ^{10}Be, ^{11}Be reaction products. The thickness of the ΔE and E silicon detectors were 75 μm and 1000 μm, respectively.

The particle identification spectrum from recoil detectors for the ^{12}B beam bombarding on the CD_2 target appears in Fig. 1. The events in these figures were selected within 150 ns timing coincidence of a light particle detected in the HELIOS PSD array. The resolution was sufficient to identify all of the Be isotopes of interest and thus discriminate different reaction channels. The corresponding light charged particles was checked by their cyclotron periods determined from the time of flight information.

The ^{11}Be in Fig. 1 were used to discriminate the ^{12}B(d,^{3}He) transition to the bound state of ^{11}Be. The ^{10}Be ions with much wider energy distribution were generated from the transition to the neutron-unbound states of ^{11}Be. With the energy loss of the escaping neutron, the average energy of ^{10}Be is around 11 MeV lower than ^{11}Be. Other possible sources of the ^{10}Be ions in Fig. 1, like the ^{12}B(d,α)^{10}Be reaction, was mostly excluded. The present setup does not allow detection of the ^{12}B(d,α) reaction to the bound state of ^{10}Be. That is why we do not see the high-energy ^{10}Be ions from the ^{12}B(d,α) reaction channel.

The the incident beam flux was monitored by the elastic scattering events on the PSD array. Elastic scattering of ^{12}B on deuterons was selected by requiring a 150-ns timing coincidence of a light particle on the PSD and a ^{12}B ions identified in the recoil detectors (see Fig. 1). The deuterons traveling for four cyclotron periods were stopped on the PSDs and their numbers were used to determine the counts of incident particles
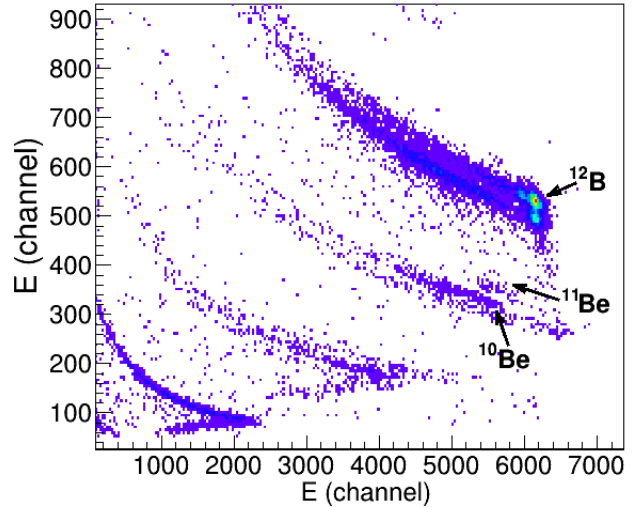

FIG. 1. The $\Delta E - E$ spectrum obtained using one of the recoil detector telescope with ^{12}B incident on the $(CD_2)_n$ target. The data shown required a coincidence with a particle in the PSD array. The particle groups labeled ^{11}Be(^{10}Be), ^{12}B are from neutron bound(unbound) states in ^{11}Be and elastic scattering of ^{12}B.

timesing the target thickness. They were divided by the calculated cross sections combining with the acceptance of the experimental setup. The deuterons were measured at an energy of 3 MeV and at an c.m. angle of $\sim 23°$, and their travelling periods were checked by the time of flight information. A variety of optical model potentials were used to calculate the elastic scattering cross sections. Uncertainties in the number of the ^{12}B beam particles timesing the target thickness varies with an r.m.s of $\sim$ 30%, depending on different optical model parameters. A procedure for determining the absolute yield is described in Section IV.

III. RESULTS

The events corresponding to the ^{12}B(d,^{3}He)^{11}Be reaction to the bound or unbound states of ^{11}Be were selected by requiring a 150$-$ns timing coincidence between a light particle in the PSD array with a ^{11}Be or ^{10}Be ion discriminated in the recoil detectors. Most of the uncorrelated background was removed by using this timing coincidence. The energies of the light particles selected using this method are plotted in Fig. 2 versus the corresponding distance where the particles were detected by the PSD detectors.

For the present range covered by the PSD array, a clear isolated bound state in ^{11}Be appears as a straight line in the plot (Fig. 2a). For the unbound states, their loci do not follow straight lines and different states merge at around $Z = 84$ cm. This is caused by the shallow orbitals
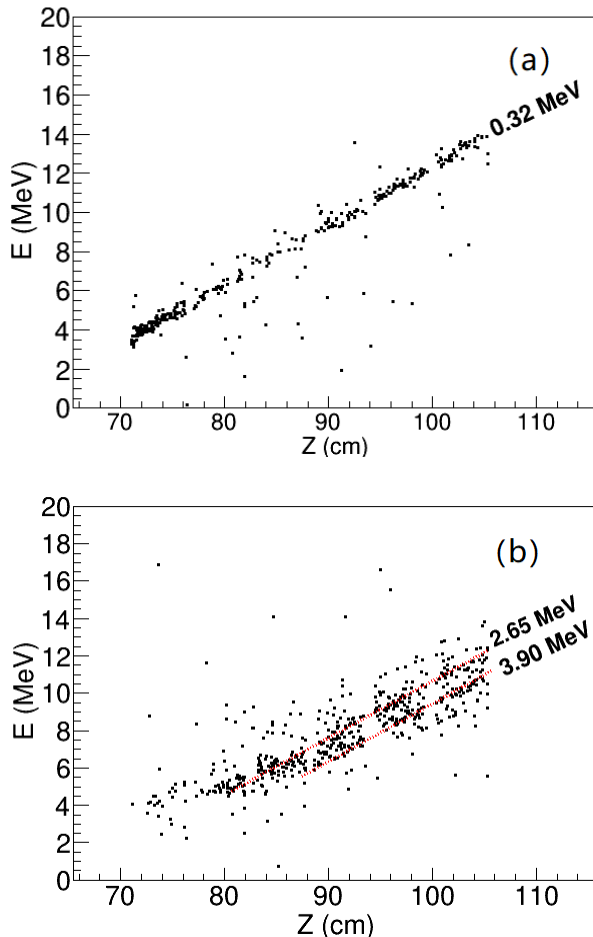
FIG. 2. Measured proton energies (E) as a function of the distance from the target (Z) for the ^{12}B(d,^{3}He)^{11}Be reaction in inverse kinematics at 12 MeV/u with a magnetic field strength of 2.3 T. The data shown required a coincidence with ^{11}Be (a) and ^{10}Be (b) in Fig. 1. Final states identified in ^{11}Be are labelled by their corresponding excitation energy. The kinematics loci for different excited states appear as diagonal red-dotted lines. See details in the text.

FIG. 3. The excitation-energy spectrum of ^{11}Be neutron bound (blue) and unbound (red) states determined from the data set as presented in Fig. 2(a) and (b) respectively. States clearly identified in the present work are labelled with their corresponding excitation energies.

of the ^{3}He particles, which reached the PSD detectors at shorter distances than the ideal situation. This effect was observed in the previous (d,^{3}He) measurement [14] as well as the kinematics calculation. The red-dotted line in Fig. 2b represents the calculated kinematics of the ideal situation where the radius of the silicon array was assumed to be zero. Events were selected where the experimental kinematics loci follows the straight lines, and were used to obtain the excitation spectrum as well as to evaluate the cross sections for the unbound states. The events obviously deviate from the straight kinematics lines were not used in the analysis.

Excitation spectra for the ^{12}B(d,^{3}He) reactions were obtained from the projection of the data along the kinematic lines and the results are shown in Fig. 3, which presents data for both neutron-bound (blue) and
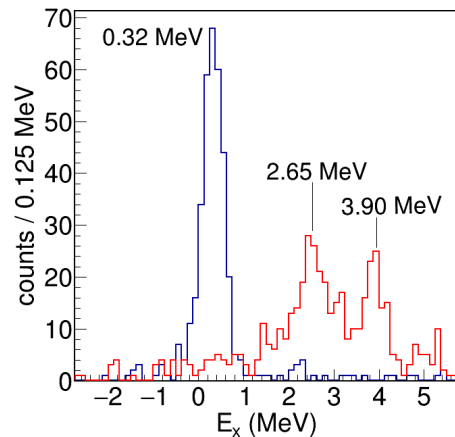
unbound (red) states. The resolution for the excitation-energy spectrum of the bound state is around 560 keV (FWHM), dominated by the energy loss of the beam and ^{3}He in the target as well as the angle straggling. The measured widths of the unbound states are also contributed to by their intrinsic widths, which are 228(21) keV for the 2.65-MeV state [5] and 3.2(8) keV for the 3.90-MeV state [15]. These widths are also compatible with the present spectrum given the appearance wider width of the 2.65-MeV state.

Table I lists the states reported in the literature for ^{11}Be [16]. Below the neutron-separation energy ($S_n = 0.510$ MeV) of ^{11}Be, the first excited state ($1/2^-$) at 320 keV was the most strongly populated state in the ^{12}B(d,^{3}He) reaction. The unbound $3/2^-$ states at 2.654 MeV also presents as a strong transition in the present reaction. The next strongly populated state probably corresponds to the one or both of the states at 3.889 MeV and 3.955 MeV. The relative contribution of these two states is discussed in Section VI. The present resolution does not allow separation of the ground state and first excited state, which are just 320 keV apart. However, an upper limit of the ground state was estimated to be 8% of the total events in the 320-keV peak, based on the standard deviation of χ^2 method. Similarly, we cannot rule out some population of the 3.410-MeV state, which was assigned as $3/2^-$ or $3/2^+$ in the previous study. An upper limit for this states was drawn to be 10% of the total events populated in the unbound states.

TABLE I. Spectroscopic factors S for the ^{12}B$(d,^3$He$)^{11}$Be reaction. The values are normalized such that the sum of S over all transitions is 3.0. Relative uncertainties on S are shown in parenthesis. Details on the uncertainties and the normalization factor is found in the text.

Literature		Present data		
E_x (MeV)	J_π	State	l	S
0.00^1	$1/2^+$			
0.32	$1/2^-$	0	$l = 1$	$0.56(12)$
1.78^1	$5/2^+$			
2.65	$3/2^-$	1	$l = 1$	$1.49(44)$
3.40^1	$3/2^{(+,-)}$			
3.89	$5/2^-$	2	$l = 1$	$0.95(27)$
3.96	$3/2^-$			
5.26^1	$5/2^-$			
6.71^1	$7/2^-$			

^{1} Not observed in the present measurement. See details in the text.

IV. ANGULAR DISTRIBUTIONS

The differential cross sections of each populated state of the ^{12}B$(d,^3$He$)^{11}$Be reaction were deduced from the present data, using the Eq. (4) in Ref. [17]. Every single PSD was either considered as a single center-of-mass angular bin or separated into two bins where the statistics allowed. The solid angle of each PSD detector is around 40 msr, and the center-of-mass angle (θ_{cm}) for a bin was determined from the reaction kinematics and the properties of HELIOS within an uncertainty of $\sim 1°$. It is noted that the acceptance of the recoiling ^{10}Be generated from the unbound states of ^{11}Be might decrease due to the breakup process. The acceptance of the ^{10}Be ions generated from the isotopic decay of ^{11}Be unbound states was calculated as a function of c.m. angles and plotted in Fig. 4. Within the range of the present data, the acceptance is mostly above 80%, and was utilized to correct the cross sections.

As stated in the experimental part, the number of the incident beam timesing the the target thickness was estimated using the elastic scattering data on the PSD array. Combining this information with solid angles of the PSDs and the counts of each state, absolute cross sections were obtained from the present analysis, as
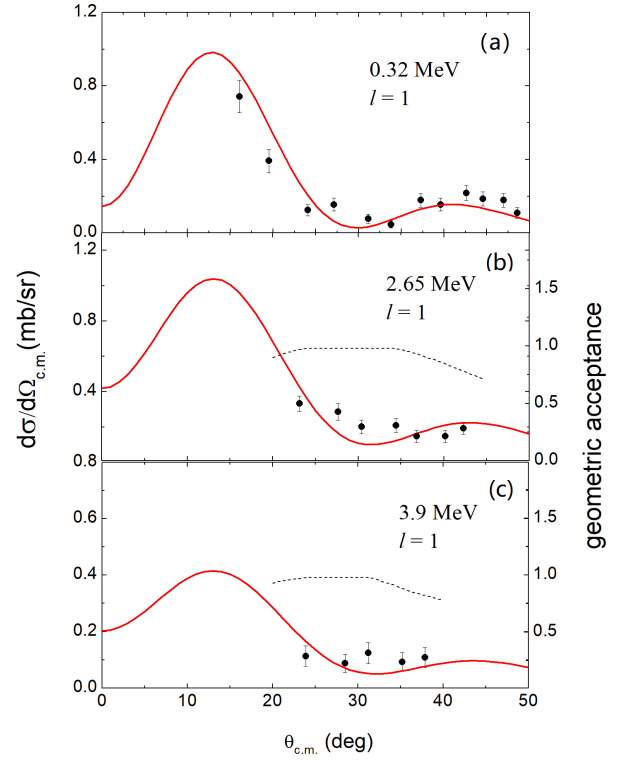

FIG. 4. Experimental(black points) and calculated(solid lines) angular distribution for the (a)0.32-, (b)2.65- and (c)3.90-MeV transition in the ^{12}B$(d,^3$He$)^{11}$Be reaction. The curves represent DWBA calculations for $\ell = 1$ transfer. Only statistical uncertainties are shown for the experimental data, and there is a systematic uncertainty of $\sim 30\%$ on the absolute cross section scale. The acceptance of the ^{10}Be recoils for the neutron-unbound states of ^{11}Be is plotted as dashed curves.

shown in Fig. 4. Error bars in the figure are statistical only. There is a systematic uncertainty of around 30% for the absolute cross sections, including the uncertainties from the determination of the beam particles, the target thickness and the cut on the PID spectrum. Most of the discussions in this paper focus on the relative S, so the uncertainty in the absolute cross sections has very little impact on the conclusions that are drawn based on the present work.

V. DWBA CALCULATIONS

The spectroscopic factors were extracted from the differential cross sections through a DWBA analysis calculated using the program PTOLEMY. The optical model parameter sets of An *et al.* [18] and Pang *et al.* [19] were used as the entrance and exit channels. The Argonne V_{18} [20] potential was used to define the

deuteron bound-state wave function and a Woods-Saxon potential with central potential well parameters of $r_0 = 1.25$ fm and $a_0 = 0.65$ fm, and with spin-orbit parameters of $V_{so} = 6.0$ MeV, $r_{so} = 1.1$ fm, and $a_{so} = 0.65$ fm, was used to define the final bound state proton wave function. The depth of the Woods-Saxon potential well was adjusted to reproduce the correct binding energy of each of the final proton bound states in ^{11}Be.

The calculated cross sections were normalized to the experimental angular distributions of each populated state using a standard χ^2 method. The results are presented in Fig. 4. For the 320-keV state, the DWBA calculations with $l = 1$ proton transfer reproduce the experimental angular distributions well. The 2.65-MeV and 3.89-MeV state data do not cover the most forward angular-distribution maximum due to the merged trajectories of these unbound states. Since the $l = 1$ angular distribution of the 320-keV state is well reproduced by the DWBA calculation, we fit the angular distributions of the 2.65-MeV and 3.89-MeV state for the experimental angular range, and larger uncertainties were determined for these states using various optical model potentials. The extracted spectroscopic factors (S) and their corresponding strengths $(GS = S)$ are listed in Table I.

A variety of optical model potentials [18, 19, 21–25] have been applied to the entrance and exit channels of the DWBA calculations to estimate uncertainties in S. For the relative S, the uncertainties arise from the statistics, the fitting procedure, and variations in the DWBA analysis, with the sum of them being $\sim 10\%$ for the 320-keV state and $\sim 20\%$ for the 2.654-MeV and 3.889-MeV states.

VI. NORMALIZATION OF THE *GS*

In the present analysis, the observed $\pi 0p_{3/2}$ strengths have been normalized to the occupancy of the orbital using the Macfarlane and French sum rule [26]. In a simple single-particle picture, the sum of the GS was normalized to 3, the occupancy of the $0p3/2$ and $0p1/2$ orbital, and the 320-keV, 2.654- and 3.899-MeV state were included in the normalization sum. The GS from higher negative excited states, like the 5.255-MeV state $(5/2^-)$, were assumed to be much smaller than these three states, which was supported by the shell model calculation (Section IV). This normalization results in a normalization factor of 0.73(26), and the uncertainty was attributed from the absolute cross sections and different optical model potentials.

The entire procedure for the extraction and normalization of the S was checked using the ^{11}B$(d,^3$He$)$ data at 13.5 MeV/u taken with the same setup. We have obtained normalized spectroscopic factors of 0.61(6), 2.09(21) and 0.30(6) for the g.s., 2_1^+ and 2_2^+ state, using the same optical model parameters stated above. These results are consistent with those reported in Ref. [27].

VII. DISCUSSION

There are three major peaks that were strongly populated in this reaction, corresponding to the $1/2^-$ at 0.32 MeV, the $3/2_1^-$ at 2.65 MeV, and the doublet at around 3.9 MeV. The population of these states should correspond to removal of one $0p_{3/2}$ orbital proton from the ground state of ^{12}B. The ground state of ^{12}B is dominated by the p-shell neutron configuration with a very little sd-shell configuration [9–11]. Further, one-proton removal reaction on ^{13}C [9, 10, 28] indicates the ^{12}B(g.s.) configuration is mostly $\pi(0p3/2)^3\nu(0p1/2)$. In principle, these strongly populated states are expected to be dominated by a configuration of $\pi(0p_{3/2})^2\nu(0p_{1/2})^1$. The pair of protons in the $0p_{3/2}$ orbital could couple into 0^+ and 2^+. The states in ^{11}Be with a $\pi(0p_{3/2})^2\nu(0p_{1/2})^1$ configuration can thus carry spin-parity of $1/2^-$, $3/2^-$ or $5/2^-$. In general, these negative-parity states are possibly dominated by two major neutron configurations, that is, the configuration within the p-shell orbitals $(0\hbar\omega)$, and with two neutrons excited to the sd-shell $(2\hbar\omega)$. The present reaction will selectively populate states with a dominant $0\hbar\omega$ configuration.

The first excited state at 0.32 MeV is expected to be dominated by the p-wave neutron configuration. This was confirmed by the one-neutron transfer reaction ^{10}Be$(d,p)^{11}$Be [29], which gives a large spectroscopic factor $(S = 0.62(4))$ for the $l = 1$ neutron component in this state. The first $3/2^-$ state at 2.65 MeV was previously seen in the (t,p) reaction [5] and β-decay of ^{11}Li [6], suggesting a normal p-shell neutron configuration. Our result confirmed these observations. The state at 3.889 MeV was previously assigned as $3/2^+$ in the ^{9}Be$(t,p)^{11}$Be reaction measurement. However, the β-delayed decay study revised the spin-parity of this state as $5/2^-$. Regarding the likely strong population of this state in the present measurement, our results support the $5/2^-$ negative-parity assignment.

There are also some negative-parity states indicating dominant intruder configuration to the sd-shell orbitals. The $3/2_2^-$ state at 3.955 MeV should not be strongly populated in the present measurement, because it is suggested to be dominated by a configuration of ^{9}Be$\otimes(sd^2)_{(2^+)}$ experimentally (see Table I in Ref. [30]) as well as in the shell model calculation (see the next subsection). The situation is similar for the $5/2_2^-$ state at 5.26 MeV.

In the following subsection, the effective-interaction shell-model, Nilsson-model, VMC and No-core shell-model will be discussed and compared with the experiments to clarify some of these ambiguities.

A. Shell model calculations

We have performed the shell model calculations for ^{12}B and ^{11}Be with the WBP interaction and recently

TABLE II. Excitation energies E_x and spectroscopic factors S for the ^{12}B$(d,^3$He$)^{11}$Be reaction calculated using the YSOX interaction [31] and Nilsson model [3]. The values are normalized such that the sum of S over all transitions is 3.0.

^{11}Be	YSOX		WBP		Nilsson	
J_π	E_x (MeV)	S	E_x (MeV)	S	E_x (MeV)	S
$1/2^+$	0.00	0.003	0.0	0.002		
$1/2^-$	0.897	0.613	-0.751	0.580	0.125	1.5
$5/2^+$	1.355	0.004	0.853	0.001		
$3/2_1^-$	3.091	1.481	0.947	0.909	2.375	1.2
$3/2^+$	3.994	< 0.001	3.232	< 0.001		
$3/2_2^-$	4.636	0.265	3.090	0.843		
$5/2_1^-$	4.918	0.633	2.845	0.668	3.569	0.3
$5/2_2^-$	6.105	< 0.001	5.495	< 0.001		
$7/2_1^-$	6.671	< 0.001	6.496	< 0.001		
$7/2_2^-$	9.365	< 0.001	7.219	< 0.001	8.875	

developed YSOX interaction [31]. The calculations assume ^{4}He as an inert core, and particles could occupy the $0p_{1/2}$, $0p_{3/2}$, $1s_{1/2}$, $0d_{5/2}$ and $0d_{3/2}$ orbitals. The calculated ^{11}Be excitation energies and corresponding spectroscopic factors S are given in Table II. Further information about the occupation number of each orbital can be found in Table III. The YSOX interaction reproduces well the ground-state energies, energy levels, electric quadrupole properties, and spin properties for most nuclei in the full psd model space including $(0-3)\hbar\omega$ excitations [31]. The level order of the ground state and first excited state is inverted in the calculation using the WBP interaction while it is well reproduced using the YSOX interaction. We will focus the discussion with calculations using the YSOX interaction.

According to the calculations using the YSOX interaction, the spectroscopic factors to the $1/2^+$ and $5/2^+$ states can be neglected in the ^{12}B$(d,^3$He$)^{11}$Be reaction. The $1/2^-$, $3/2_1^-$ and $5/2_1^-$ states have large overlaps with the ^{12}B g.s., corresponding to the experimentally observed states at 320 keV, 2.654 MeV, and 3.899 MeV. These states have a configuration with one particle in $0p_{1/2}$ orbital, with very little excitation to the sd shell, consistent with our previous discussion. The calculated S (Table III) of the former two states are in reasonable agreement with the experimental values. The $3/2_2^-$ state in the calculation probably corresponds to the 3.955-MeV state, and it is dominated by a $2\hbar\omega$ configuration, which has a very small overlap with the ^{12}B g.s. The S of the $3/2_2^-$ and the $5/2_1^-$ state are added and compared with the experimental spectroscopic factor of the doublet around 3.9 MeV, showing reasonable agreement. It worth noting that the experimentally observed events at around 3.9 MeV should be dominated by the 3.899-MeV state, with a smaller contribution from the 3.955-MeV state due to the configuration mixing of

the $0\hbar\omega$ excitation.

The maximum angular momentum that can be obtained within the p-shell orbitals is $7/2^-$. However, the present reaction will not populate it because of the $l = 1$ transferred angular momentum. We also listed the shell model calculation for the first two $7/2^-$ states in Table II and III for comparison.

There is another $5/2^-$ state at around 6 MeV in the calculation, with a $2\hbar\omega$ configuration, which probably corresponds to the previously observed 5.255-MeV state in the ^{9}Be(t,p) reaction [5]. This state could not be observed in the present measurement due to the acceptance of the setup. However, the calculated spectroscopic factor for this state is much smaller than the $5/2_1^-$ state or the $3/2_1^-$ states, indicating the p-wave strength observed in this measurement could account for most of the proton removal strengths in the $0p_{3/2}$ orbital, and it is reasonable to normalize the sum of them to the occupancy of the $0p_{3/2}$ orbital in the ^{12}B g.s. For another, there is no strong indication of another low-lying $3/2^-$ state with $2\hbar\omega$ configuration in the calculation, in contrast to the previous suggestion for the 3.410-MeV state in the (t,p) reaction.

B. Nilsson model calculations

Here we understand the structure of the neutron-rich Be isotopes within the Nilsson model to study their collective degree of freedom. Within this framework, the $1/2_1^-$, $3/2_1^-$ and $5/2_1^-$ are band members of $K^\pi = 1/2^-$, and using [32]

$$E_x(J) = \frac{\hbar^2}{2\Theta} \cdot [J(J+1) + a \cdot (-1)^{J+1/2} \cdot (J+1/2)] + E_0, \quad (1)$$

their excitation energies were calculated with the band parameter $b = \hbar/2\Theta = 0.5$ MeV and the Coriolis decoupling parameter $a = 0.5$. This band is expected to be terminated by the $7/2^-$ state with all the angular momentum of the valence nucleons aligned. It appears that the second $7/2^-$ state in Table II belongs to this band due to its dominant configuration within the p-shell. The first $7/2^-$ probably corresponds to the member of the long 2α-cluster band, which were understood as dominant by $2\hbar\omega$ configurations in the shell-model picture. Within the Nilsson scheme, the $Z = 5$ proton is expected to occupy the $3/2[101]$ level and the g.s. of ^{12}B belong to band with $K^\pi = 1^-$. Since the level parentage is attributed only to the $0p_{3/2}$ orbit, the spectroscopic factors depend only on the Clebsch-Gordan coefficients according to Eq. 3 of Ref. [3], and we predict the S as listed in Table II, which were also normalized to the occupancy of the orbitals.

TABLE III. Shell-model occupation numbers for ^{12}B and ^{11}Be with the YSOX interaction.

		Protons					Neutrons				
J_π	E_x (MeV)	$0p_{3/2}$	$0p_{1/2}$	$0d_{5/2}$	$0d_{3/2}$	$0s_{1/2}$	$0p_{3/2}$	$0p_{1/2}$	$0d_{5/2}$	$0d_{3/2}$	$0s_{1/2}$
1^+	^{12}B g.s.	2.701	0.193	0.04	0.052	0.014	3.733	1.117	0.071	0.061	0.018
$1/2^+$	0.00	1.747	0.222	0.009	0.017	0.005	3.459	0.483	0.227	0.04	0.792
$1/2_1^-$	0.897	1.8	0.162	0.009	0.025	0.005	3.85	1.05	0.05	0.042	0.009
$5/2^+$	1.355	1.71	0.259	0.01	0.017	0.004	3.442	0.502	0.859	0.061	0.137
$3/2_1^-$	3.091	1.797	0.148	0.015	0.03	0.009	3.374	1.138	0.294	0.061	0.133
$3/2^+$	3.994	1.697	0.269	0.012	0.018	0.005	3.388	0.552	0.244	0.208	0.608
$3/2_2^-$	4.636	1.658	0.314	0.01	0.015	0.004	2.935	0.545	0.718	0.125	0.677
$5/2_1^-$	4.918	1.769	0.179	0.019	0.026	0.007	3.788	1.027	0.095	0.055	0.035
$5/2_2^-$	6.105	1.624	0.356	0.006	0.011	0.003	2.675	0.41	1.032	0.176	0.792
$7/2_1^-$	6.671	1.629	0.343	0.008	0.016	0.004	2.614	0.418	1.145	0.233	0.59
$7/2_2^-$	9.365	1.884	0.041	0.029	0.036	0.01	2.919	1.693	0.063	0.239	0.086

C. VMC calculation

(to be continued)

D. No-core shell-model calculation

(to be continued)

E. Comparisons

The ^{11}B$(d,^3$He$)^{10}$Be reaction also serves as another testing ground for the Nilsson model. Information could be obtained from previous data as well as the stable beam data in the present experiment. Both measurement agree on spectroscopic factors of around 0.6(6) and 2.1(21) for the 0_1^+ and 2_1^+ states. In order to further understand the experimental results, we also compare the experimental spectroscopic factors of the ^{11}B$(d,^3$He$)^{10}$Be to the calculated ones of shell model using the YOSX interaction as well as Nillson model. Fig. 5 represents these calculated spectroscopic factors and excitation energies in comparison with the experiments, for the $1/2_1^-$, $3/2_1^-$, $5/2_1^-$ states of ^{11}Be in the ^{12}B$(d,^3$He$)^{11}$Be reaction and 0_1^+ and 2_1^+ states of ^{10}Be in the ^{11}B$(d,^3$He$)^{10}$Be reaction. Excitation energies of the 2^+ state of ^{10}Be in the Nilsson model was calculated using $b = 0.59$. Although the Nilsson model reproduces their energies, the spectroscopic factors are underestimated for the $3/2_1^-$, $5/2_1^-$ states in ^{11}Be and 2_1^+ state in ^{10}Be.

Experimental and theoretical studies hinted on the possible existence of the $N = 6$ shell closures in ^{8}He [33] and ^{14}O [34, 35]. More recently, various sides of evidences for the $Z = 6$ shell closure in $^{13-20}$C has been reported [36]. If we assume that $N = 6$ is a subshell, the $1/2_1^-$, $3/2_1^-$ and $5/2_1^-$ states could be viewed as composed of one neutron in $0p_{1/2}$ orbital outside the ^{10}Be(0^+) or ^{10}Be(2^+) core. The $2j + 1$ weighted energy centroid of $3/2_1^-$ and $5/2_1^-$ states (shown as dashed red line in Fig. 5) compared to $1/2_1^-$ state in ^{11}Be is close to the energy difference of 2_1^+ and 0_1^+ states in ^{10}Be. Further, the spectroscopic factors of $1/2_1^-$ state and the sum of $3/2_1^-$ and $5/2_1^-$ states are close to the values of 0_1^+ and 2_1^+ states for the ^{11,12}B$(d,^3$He$)$ transition, respectively (see Fig. 5). The situation is similar in the shell model calculations using YSOX interaction. Spectroscopic study of the negative-parity states populated in the proton removal reactions on ^{11,12}B shows a consistent picture, with the valence neutron in the $0p_{1/2}$ orbital coupling to the ^{10}Be core.
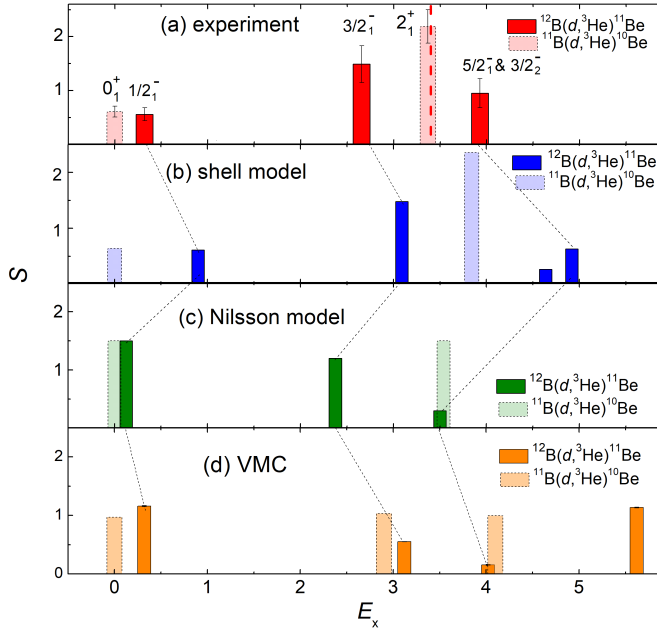
VIII. SUMMARY

FIG. 5. The experimental (a) and calculated (b,c,d) excitation energies and spectroscopic factors of the $1/2_1^-$, $3/2_1^-$, $5/2_1^-$ states of ^{11}Be ^{12}B$(d,^3$He$)^{11}$Be reaction and 0_1^+ and 2_1^+ state of ^{10}Be in the ^{11}B$(d,^3$He$)^{10}$Be reaction. (b), (c) and (d) were calculated using shell model with YSOX interaction, Nilsson model and VMC method, respectively. The error bars for the experimental values are just for relative S. The dashed line in (a) is the $2j+1$ weighted energy centroid of $3/2_1^-$ and $5/2_1^-$ states in ^{11}Be.

[1] H. G. Bohlen, W. von Oertzen, R. Kalpakchieva, T. N. Massey, T. Dorsch, M. Milin, C. Schulz, T. Kokalova, and C. Wheldon, Journal of Physics: Conference Series **111**, 012021 (2008).

[2] H. Bohlen, R. Kalpakchieva, W. von Oertzen, T. Massey, B. Gebauer, S. Grimes, T. Kokalova, H. Lenske, A. Lenz, M. Milin, C. Schulz, S. Thummerer, S. Torilov, and A. Tumino, Nuclear Physics A **722**, C3 (2003).

[3] A. O. Macchiavelli, H. L. Crawford, C. M. Campbell, R. M. Clark, M. Cromaz, P. Fallon, M. D. Jones, I. Y. Lee, and M. Salathe, Phys. Rev. C **97**, 011302 (2018).

[4] D. Santiago-Gonzalez, K. Auranen, M. L. Avila, A. D. Ayangeakaa, B. B. Back, S. Bottoni, M. P. Carpenter, J. Chen, C. M. Deibel, A. A. Hood, C. R. Hoffman, R. V. F. Janssens, C. L. Jiang, B. P. Kay, S. A. Kuvin, A. Lauer, J. P. Schiffer, J. Sethi, R. Talwar, I. Wiedenhöver, J. Winkelbauer, and S. Zhu, Phys. Rev.

Lett. **120**, 122503 (2018).

[5] G.-B. Liu and H. T. Fortune, Phys. Rev. C **42**, 167 (1990).

[6] Y. Hirayama, T. Shimoda, H. Izumi, A. Hatakeyama, K. Jackson, C. Levy, H. Miyatake, M. Yagi, and H. Yano, Physics Letters B **611**, 239 (2005).

[7] D. Morrissey, K. McDonald, D. Bazin, B. Brown, R. Harkewicz, N. Orr, B. Sherrill, G. Souliotis, M. Steiner, J. Winger, S. Yennello, B. Young, S. Lukyanov, G. Chubarian, and Y. Oganessian, Nuclear Physics A **627**, 222 (1997).

[8] N. Aoi, K. Yoneda, H. Miyatake, H. Ogawa, Y. Yamamoto, E. Ideguchi, T. Kishida, T. Nakamura, M. Notani, H. Sakurai, T. Teranishi, H. Wu, S. Yamamoto, Y. Watanabe, A. Yoshida, and M. Ishihara, Nuclear Physics A **616**, 181 (1997), radioactive Nuclear Beams.

[9] G. Mairle, L. K. Pao, G. J. Wagner, K. T. Knöpfle, and

H. Riedesel, Zeitschrift für Physik A Atoms and Nuclei **301**, 157 (1981).

[10] J. Lind, G. Garvey, and R. Tribble, Nuclear Physics A **276**, 25 (1977).

[11] H. Y. Lee, J. P. Greene, C. L. Jiang, R. C. Pardo, K. E. Rehm, J. P. Schiffer, A. H. Wuosmaa, N. J. Goodman, J. C. Lighthall, S. T. Marley, K. Otsuki, N. Patel, M. Beard, M. Notani, and X. D. Tang, Phys. Rev. C **81**, 015802 (2010).

[12] A. Wuosmaa, J. Schiffer, B. Back, C. Lister, and K. Rehm, Nucl. Instr. Meth. Phys. Res. Sect. A **580**, 1290 (2007).

[13] J. Lighthall, B. Back, S. Baker, S. Freeman, H. Lee, B. Kay, S. Marley, K. Rehm, J. Rohrer, J. Schiffer, D. Shetty, A. Vann, J. Winkelbauer, and A. Wuosmaa, Nucl. Instr. Meth. Phys. Res. Sec. A **622**, 97 (2010).

[14] S. Bedoor, A. H. Wuosmaa, M. Albers, M. Alcorta, S. Almaraz-Calderon, B. B. Back, P. F. Bertone, C. M. Deibel, C. R. Hoffman, J. C. Lighthall, S. T. Marley, D. G. Mcneel, R. C. Pardo, K. E. Rehm, J. P. Schiffer, and D. V. Shetty, Phys. Rev. C **93**, 044323 (2016).

[15] H. T. Fortune, Phys. Rev. C **86**, 037302 (2012).

[16] J. Kelley, E. Kwan, J. Purcell, C. Sheu, and H. Weller, Nuclear Physics A **880**, 88 (2012).

[17] C. R. Hoffman, B. B. Back, B. P. Kay, J. P. Schiffer, M. Alcorta, S. I. Baker, S. Bedoor, P. F. Bertone, J. A. Clark, C. M. Deibel, B. DiGiovine, S. J. Freeman, J. P. Greene, J. C. Lighthall, S. T. Marley, R. C. Pardo, K. E. Rehm, A. Rojas, D. Santiago-Gonzalez, D. K. Sharp, D. V. Shetty, J. S. Thomas, I. Wiedenhöver, and A. H. Wuosmaa, Phys. Rev. C **85**, 054318 (2012).

[18] H. An and C. Cai, Phys. Rev. C **73**, 054605 (2006).

[19] D. Y. Pang, P. Roussel-Chomaz, H. Savajols, R. L. Varner, and R. Wolski, Phys. Rev. C **79**, 024615 (2009).

[20] R. B. Wiringa, V. G. J. Stoks, and R. Schiavilla, Phys. Rev. C **51**, 38 (1995).

[21] Y. Han, Y. Shi, and Q. Shen, Phys. Rev. C **74**, 044615 (2006).

[22] W. W. Daehnick, J. D. Childs, and Z. Vrcelj, Phys. Rev. C **21**, 2253 (1980).

[23] R. Varner, W. Thompson, T. McAbee, E. Ludwig, and T. Clegg, Physics Reports **201**, 57 (1991).

[24] J. Lohr and W. Haeberli, Nuclear Physics A **232**, 381 (1974).

[25] C.-T. Liang, X.-H. Li, and C.-H. Cai, Journal of Physics G: Nuclear and Particle Physics **36**, 085104 (2009).

[26] M. H. Macfarlane and S. C. Pieper, *Report ANL-76-11, Rev. 1, 1978 (unpublished)*, .

[27] U. Schwinn, G. Mairle, G. J. Wagner, and C. Rämer, Zeitschrift für Physik A Atoms and Nuclei **275**, 241 (1975).

[28] D. Scott, P. Portner, J. Nelson, A. Shotter, A. Mitchell, N. Chant, D. Montague, and K. Ramavataram, Nuclear Physics A **141**, 497 (1970).

[29] K. T. Schmitt, K. L. Jones, A. Bey, S. H. Ahn, D. W. Bardayan, J. C. Blackmon, S. M. Brown, K. Y. Chae, K. A. Chipps, J. A. Cizewski, K. I. Hahn, J. J. Kolata, R. L. Kozub, J. F. Liang, C. Matei, M. Matoš, D. Matyas, B. Moazen, C. Nesaraja, F. M. Nunes, P. D. O'Malley, S. D. Pain, W. A. Peters, S. T. Pittman, A. Roberts, D. Shapira, J. F. Shriner, M. S. Smith, I. Spassova, D. W. Stracener, A. N. Villano, and G. L. Wilson, Phys. Rev. Lett. **108**, 192701 (2012).

[30] H. T. Fortune and R. Sherr, Phys. Rev. C **83**, 054314 (2011).

[31] C. Yuan, T. Suzuki, T. Otsuka, F. Xu, and N. Tsunoda, Phys. Rev. C **85**, 064324 (2012).

[32] A. Bohr and B. R. Mottelson, *R 1998 Nulear Struture, vol. II, p. 33, World Sientific, Singapore*, .

[33] F. Skaza, V. Lapoux, N. Keeley, N. Alamanos, E. C. Pollacco, F. Auger, A. Drouart, A. Gillibert, D. Beaumel, E. Becheva, Y. Blumenfeld, F. Delaunay, L. Giot, K. W. Kemper, L. Nalpas, A. Obertelli, A. Pakou, R. Raabe, P. Roussel-Chomaz, J.-L. Sida, J.-A. Scarpaci, S. Stepantsov, and R. Wolski, Phys. Rev. C **73**, 044301 (2006).

[34] I. Angeli and K. Marinova, Atomic Data and Nuclear Data Tables **99**, 69 (2013).

[35] T. Otsuka, R. Fujimoto, Y. Utsuno, B. A. Brown, M. Honma, and T. Mizusaki, Phys. Rev. Lett. **87**, 082502 (2001).

[36] D. Tran, H. Ong, and et al., Nature Communications **9**, 1 (2018).